BRIEF COMMUNICATION

PHYSICAL ANTHROPOLOGY *American Journal of* WILEY

A critical assessment of the potential for Structure-from-Motion photogrammetry to produce high fidelity 3D dental models

Christopher Martin Silvester [ORCID] | Simon Hillson

Institute of Archaeology, University College London, London, UK

Correspondence
Christopher Martin Silvester, University College London, Institute of Archaeology, London, WC1H 0PY, UK.
Email: christopher.silvester.15@ucl.ac.uk

Abstract

Objectives: The recent proliferation of methods of 3D model generation has enabled the development of new approaches to the analysis of dental form, function and wear. This article assesses whether Structure-from-motion (SfM) photogrammetry is capable of producing virtual 3D models of teeth of adequate quality for assessing fine scale surface details, such as dental macrowear patterns. Reference models were generated using a high resolution structured light scanner to assess the accuracy of the photogrammetric models generated.

Materials and Methods: Dental gypsum models of the molar teeth of human individuals from St. Michael's Litten, Chichester, Post-medieval assemblage (*n* = 17) were used for 3D model generation. Photogrammetry was performed using Agisoft Metashape and reference 3D models were generated using a GOM ATOS 80 scanner. Focus stacking was explored as a method of enhancing 3D model detail. Differences between the photogrammetric and reference models were assessed using CloudCompare and the quality of the surface detail was examined quantitatively using Occlusal Fingerprint Analysis.

Results: Photogrammetric model generation was highly replicable and the tooth models produced closely approximated the overall geometry of those derived from the structured light scanner. Dental wear facet area measurements on the photogrammetric models differed significantly, however, from those derived from the structured light scanning reference models.

Discussion: Photogrammetry can create virtual dental models from which crude quantitative size and shape data can be obtained. Finer scale surface details are not accurately reproduced on SfM models using the methods outlined in the current article due to high levels of surface noise.

KEYWORDS
3D models, accuracy, photogrammetry, teeth, wear facets

1 | INTRODUCTION

The recent proliferation of surface scanning technologies has enabled the development of new approaches to the analysis of dental morphology and wear. Crown morphology provides important information regarding tooth function and the evolutionary development of tooth structures. Once erupted into the mouth, wear changes this morphology to produce polished facets that reflect the culmination of tooth use over a substantial period of an individual's lifetime (Kaiser et al., 2013). Virtual dental models have been used extensively to examine dental morphology, functional potential and complexity of tooth form (Allen, Cooke, Gonzales, & Kay, 2015; Bunn & Ungar, 2009; Evans, Wilson, Fortelius, & Jernvall, 2007; Glowacka et al., 2016; Klukkert, Teaford, & Ungar, 2012; Ungar, Healy, Karme, Teaford, & Fortelius, 2018). Similarly, virtual models of dental macrowear have been used to infer patterns of masticatory and non-masticatory tooth use and associated differences in dietary consistency (Fiorenza et al., 2011; Fiorenza, Benazzi, Oxilia, & Kullmer, 2018; Fiorenza & Kullmer, 2013; Koenigswald, 2018; Kullmer et al., 2009). The occlusal and inter-arch relationships of specimens damaged and deformed by taphonomic processes can also be reconstructed using virtual models (Kullmer et al., 2013), which can then be reproduced with the assistance of 3D printing technologies (Fiorenza et al., 2018). Computer-aided design and computer-aided manufacturing (CAD/CAM) systems are widely used within contemporary dental practice and can assist the analysis of specific teeth, arch form and malocclusion (Taneva, Kusnoto, & Evans, 2015).

Most studies use structured light scanning (SLS), CT scanning or laser scanning for 3D model generation. In SLS systems, the target object is illuminated by a series of alternating 2D patterns of light whilst a sensor, such as a video camera, is used to acquire images of the scene under the structured light conditions. The distortion of the projected light pattern is used to infer the underlying 3D geometry of the scene (Geng, 2011).

Structure-from-motion photogrammetry (SfM) is a method of 3D data acquisition that offers a readily available and low-cost alternative to structured light, laser or CT scanning systems as image capture only requires access to a conventional camera (Micheletti, Chandler, & Lane, 2015). In SfM, a series of overlapping photographs is taken, to cover the target object or area. Software extracts key points from the photographs through the identification of correspondences between images. This extracted database of features is used to resolve simultaneously camera position, alignment and scene geometry. An initial 3D cloud of points on the target object is generated from the reconstruction and matching of the key points in multiple photographs. Further points can then be added to this so-called sparse point cloud and transformed into a more densely defined 3D mesh representing the topography of the target object surface (Szeliski, 2011; Westoby, Brasington, Glasser, Hambrey, & Reynolds, 2012).

Photogrammetric methods have been used extensively in a variety of disciplines to generate models across a range of scales, from landscapes to small objects (Bevan et al., 2014; Hassett & Lewis-Bale, 2017; Hess, MacDonald, & Valach, 2018; James & Robson, 2012).

Several recent studies have indicated that SfM models of small objects can closely approximate the overall size and shape of virtual models generated using high resolution 3D scanners (Clini, Nespeca, Ruggeri, Frapiccini, & Mengoni, 2016; Kontogianni, Chliverou, Georgopoulos, Koutsoudis, & Pavlidis, 2017; Kontogianni, Chliverou, Koutsoudis, Pavlidis, & Georgopoulos, 2017). Within physical anthropology, it is possible to take accurate measurements of larger skeletal elements, such as crania, using photogrammetric models instead of the original specimens (Morgan, Ford, & Smith, 2019).

Concerns have however been raised over the repeatability and accuracy of SfM (Napolitano & Glisic, 2018). In addition, the quality of the visualization of fine scale details on photogrammetric models of small topographically complex objects has yet to be comprehensively assessed. Photogrammetric software finds correspondences between the parts of images that are in focus, which may lead to failure in the point matching procedure when using macro lenses with a shallow depth of field (Kontogianni, Chliverou, Koutsoudis, et al., 2017). Focus stacking has been suggested as a method to circumvent this issue (Clini et al., 2016) but will result in substantially longer image acquisition and processing times. Focus stacking involves taking a series of macro images at different focal planes. The focal plane is shifted by either moving a camera with a fixed focus on a macro rail system or by manually adjusting the focal distance. All the detail in focus within each image taken at different focal planes can then be combined to produce a composite fully focused image (Clini et al., 2016; Gallo, Muzzupappa, & Bruno, 2014). A previous study has indicated that the use of focus stacking may enhance the quality of the reproduction of small-scale surface details (Kontogianni, Chliverou, Georgopoulos, et al., 2017).

The current study aimed to investigate the quality and fidelity of 3D dental models generated using SfM. The repeatability of SfM model generation was examined alongside the deviation of each dental model from a reference virtual model generated using a high resolution SLS system. Focus stacked structure-from-motion photogrammetry (FS-SfM) was also assessed as a method of enhancing 3D dental model fidelity. The quality of the reproduction of fine object details was quantified by examining and comparing dental macrowear patterns between the virtual models produced using each method.

2 | MATERIALS AND METHODS

2.1 | Materials

Human specimens were selected from the St. Michael's Litten, Chichester, Post-medieval assemblage (n = 17) held at the Institute of Archeology, University College London. Surface scan data cannot be effectively derived directly from the teeth due to the reflective and lustrous qualities of enamel (Errickson et al., 2017; Fiorenza, Benazzi, & Kullmer, 2009), therefore, a dental gypsum model was produced of each specimen. An impression was taken of the best preserved mandibular molar row of each specimen using a two-phase,

two-step, putty-wash technique (President® Coltène/Whaledent Inc.) and a dental gypsum model was produced (Suprastone® Dental Die Stone Type IV; Kerr Corporation).

2.2 | Structure-from-Motion: Photography and model generation

Several factors impact the quality and resolution of the final 3D models produced by SfM and require consideration when developing a strategy for image acquisition (James & Robson, 2014; Morgan, Brogan, & Nelson, 2017; Mosbrucker, Major, Spicer, & Pitlick, 2017). The resolution of the final 3D model produced is directly dependent upon the surface texture of the target object, therefore, highly textured objects with images taken at higher resolutions will result in the best models (Salvi, Fernandez, Pribanic, & Llado, 2010). Surface texture refers to the pattern or structure on a surface and is dependent upon localized variability in the reflection and geometric properties of an object (Luhmann, Robson, Kyle, & Boehm, 2013).

Greater numbers of photographs that are convergent upon the target object and have maximized overlap increase the redundancy of the key point correspondences identified between images and enhance the final resolution of the model (James & Robson, 2014; Westoby et al., 2012). Illumination should be diffuse to avoid intense shadows that might result in holes in the final point cloud (Mosbrucker et al., 2017). Model generation conducted using subsets of images of decreasing number indicated that improvements in point cloud density were not marked when using >100 images, whereas, a steep decrease in point cloud density occurred in image sets of <70 images. Consequently, 80 images were captured of each dental model when performing conventional SfM using a custom-built camera rig to ensure that the sequence of image capture was consistent between specimens (Figure 1). The angle between image captures during turntable revolutions was 22.5^0 for each of the five camera positions used. Camera settings were kept constant to improve the camera calibration model (Table 1) and followed the recommendations of Mosbrucker et al. (2017).

The photographs were imported into Agisoft Metashape Professional Edition (v.1.5.5) and a standard workflow was developed
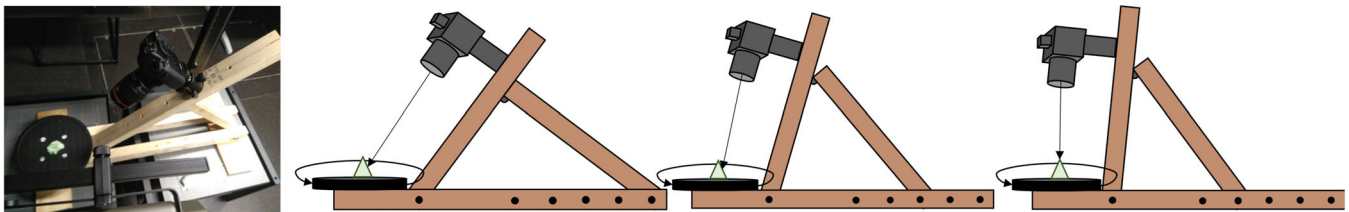

FIGURE 1 Illustration of the camera rig used for image capture. The camera was positioned on an adjustable arm that could be raised and lowered to achieve an angle of incidence to the turntable of 2°, 12°, 21°, 31°, and 45°. Sixteen images were taken at each camera position whilst the dental model was rotated on a black turntable (angle between convergent photographs was 22.5°)

TABLE 1 The camera settings used during image capture in the current study for the generation of 3D models using conventional Structure-from-Motion photogrammetry and Focus Stacked Structure-from-Motion photogrammetry

Setup	Normal SfM	Focus stacked SfM
Camera	Canon EOS6D (20.2megapixels)	Canon EOS6D (20.2megapixels)
Lens	100 mm canon EF macro lens	65 mm canon MP-E macro lens
Number of images	80 16 per turntable revolution with 5 different camera positions	20–30 images per camera position were taken and imported into helicon focus 30 full-focus composite images produced per dental model to achieve full coverage
Aperture F-number	11	2.8
Shutter speed	1/40s	1/2000s
ISO	100	100
Lighting	Copy stand used to provide consistent non-directional ambient light	Copy stand used to provide consistent non-directional ambient light
Image format	RAW	JPG
Scale	4 Agisoft Metashape coded markers distributed around the target object provided known distances for scaling the 3D model. The markers spanned the full area to be reconstructed in order to provide more accurate scaling.	Several coded markers (2 mm in size) with a clearly defined centroid were fixed adjacent to the tooth to provide known distances for scaling the 3D model.

(Figure 2). Structure-from-Motion photogrammetry has a tendency to produce an uneven distribution of points in the final point cloud and often incorporates high levels of redundancy (Hassett & Lewis-Bale, 2017). Therefore, a protocol for cleaning the sparse point cloud in
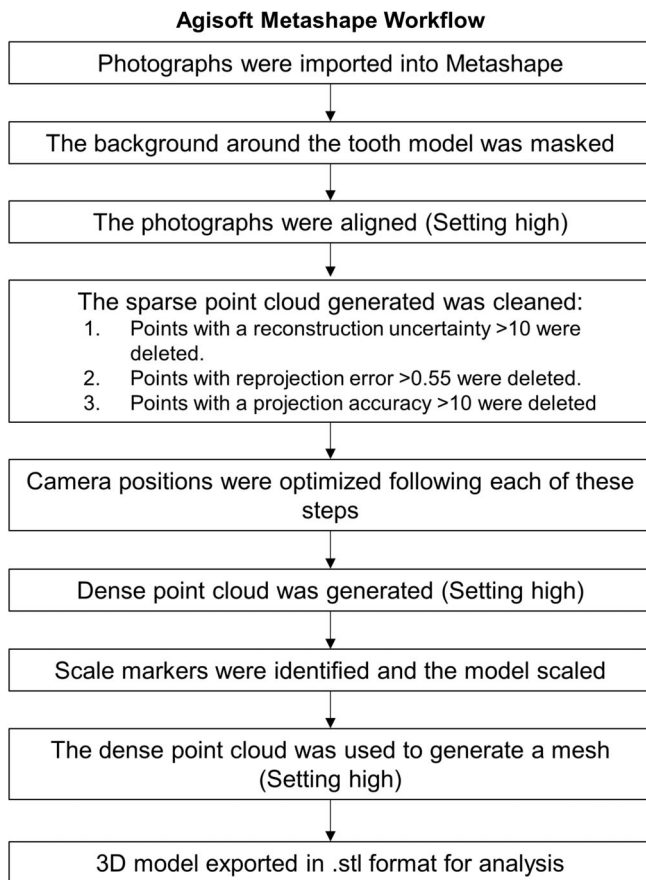
Agisoft Metashape Workflow

Photographs were imported into Metashape

↓

The background around the tooth model was masked

↓

The photographs were aligned (Setting high)

↓

The sparse point cloud generated was cleaned:
1. Points with a reconstruction uncertainty >10 were deleted.
2. Points with reprojection error >0.55 were deleted.
3. Points with a projection accuracy >10 were deleted

↓

Camera positions were optimized following each of these steps

↓

Dense point cloud was generated (Setting high)

↓

Scale markers were identified and the model scaled

↓

The dense point cloud was used to generate a mesh (Setting high)

↓

3D model exported in .stl format for analysis

FIGURE 2 Agisoft Metashape Workflow used for Structure-from-Motion model generation in the current paper. All operations were performed on high settings

Agisoft Metashape was developed to enhance the accuracy of the final reconstructed object surface and reduce reprojection error (Delaunoy, Prados, Piracés, Pons, & Sturm, 2008; Gargallo, Prados, & Sturm, 2007). Model generation was conducted on a computer with 64 GB of RAM, a 4.20 GHz processor and a separate 8 GB graphics card. The 3D models generated were exported in .stl format for analysis.

Image capture for focus stacking was performed using a Canon EOS6D with a Canon MP-E 65 mm lens mounted on a StackShot macro rail system (Cognisys, Inc.) (Table 1). The focal plane was shifted 650 μm between consecutive images using the macro rail. Each stack of images was combined using Helicon Focus Pro (v. 7.8.5) to produce a full focus composite image for each camera position. As images were captured in a sequential order, the depth-map approach was used for composite image generation. The software locates the source image in which the sharpest pixel is present and this pixel is used to produce the composite full focus image (HeliconSoft, 2019; Kontogianni, Chliverou, Georgopoulos, et al., 2017). The composite focused images were then imported into Agisoft Metashape and the standard workflow for 3D model generation was used (Figure 2). FS-SfM 3D model generation was performed for nine specimens due to the time intensive character of image capture (Table 2).

2.3 | Structured light scanning (SLS)

Reference 3D dental models were generated using a structured light scanning system (GOM ATOS 80 Scanner, GOM, Braunschweig, Germany). The scanning system uses a blue light projector, to better filter out ambient light, and a stereo pair of cameras. Each dental model was mounted onto the robotic arm of the scanner using a magnet and zinc-coated steel washer glued to the base of the dental model. The GOM scanner offers a minimum point-to-point spacing of 30 μm. Data acquired was imported directly into ATOS professional (v 2018 Hotfix 3) and then converted into a polygonal mesh, which could be exported in .stl format for analysis

TABLE 2 The time taken to perform surface data acquisition and 3D model generation for each method used

Method of 3D model generation	Surface data acquisition and 3D model generation	Time taken (minutes)	Total (minutes)
Structured light scanning	Scanning of dental model	10	15
	Polygonise data and export model	5	
Normal photogrammetry	Photographic capture of dental model (80 images)	20	100
	Agisoft: Align photos	5	
	Agisoft: Depth map and dense cloud generation	70	
	Agisoft: Build mesh and export model	5	
Focus stacked photogrammetry	Photographic capture of dental model (30 views with stacks averaging 23 photographs)	120	180
	Focus-stacking of images in helicon	30	
	Agisoft: Align photos	5	
	Agisoft: Depth map and dense cloud generation	10	
	Agisoft: Build mesh and export model	15	

2.4 | Comparison of virtual model dimensions and surface detail

A repeatability study was conducted to investigate the consistency with which SfM can generate 3D models of the same object when the sequence of image capture is closely replicated. The process of SfM image capture and model generation was conducted twice for three dental models from the St. Michael's Litten assemblage. Repeated image capture was performed on separate days. Following 3D model generation, the two-point clouds for each specimen were aligned and the distances between the two-point clouds measured using CloudCompare software (v 2.9.1). The same protocol was followed to determine how closely the SfM and FS-SfM models approximated the overall geometry of the 3D SLS generated reference models.

Occlusal Fingerprint Analysis (OFA), a method of dental macrowear analysis developed by Kullmer et al. (2009), was used to assess quantitatively the quality of the reproduction of dental wear facets on the occlusal surface of the tooth (Figure 3). Dental wear facets are shiny planar surfaces with well-defined edges which chiefly result from dental attrition; tooth-tooth contact mediated by a thin layer of intervening particles and saliva (Kaidonis, 2008). It has

been argued that a virtual model resolution of at least 60 μm is required to effectively analyze dental wear facet patterns (Kullmer et al., 2009). Dental wear facets were identified on corresponding SfM (n = 17), FS-SfM (n = 9) and SLS virtual models (n = 17). Their 3D area was calculated and compared in GOM Inspect (v 2018 Hotfix 3). Cross-sectional areas of crowns were also calculated in GOM Inspect by creating a best-fit plane using the cervix of the tooth and then translating it to the deepest point of the occlusal fissure system, usually the base of the central fossa. A section was then created through the tooth at this level and its area measured (Figure 3) (M'Kirera & Ungar, 2003; Ulhaas, Kullmer, Schrenk, & Henke, 2004).

Measurements were compared using the Bland–Altman approach (Bland & Altman, 1986). Close agreement would be indicated by a mean difference between measurements close to 0 and 95% limits of agreement that are small relative to the magnitude of the measurements being taken. Percentage error was calculated for each comparison to describe the relationship between the magnitude of the measurement and the error in the measurement. Paired sample t-tests and repeated-measures ANOVA were used to determine whether any differences in measurement were significant. Statistical analysis was
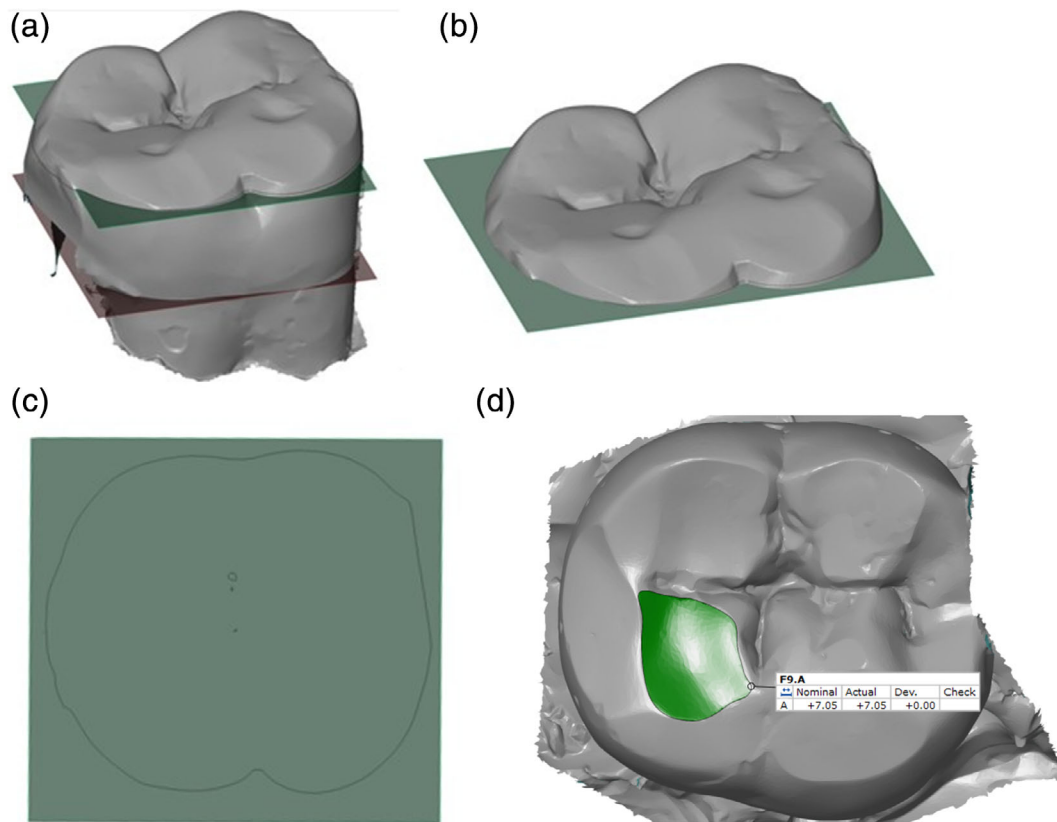

FIGURE 3 Process for calculating cross-sectional crown area and wear facet areas using GOM Inspect. Crown area was calculated by translating a reference plane (red) fitted to the cervix of the tooth along the z-axis to the deepest point of the occlusal surface (green) (a). In teeth that have been digitally cut from the tooth row, the mesial and distal surfaces are frequently absent from the polygonal model and must be digitally reconstructed. The polygonal model is then cut at the level of the occlusal plane (b). The 2D area of the tooth is measured at the level of the occlusal plane (c). Wear facet area is derived by outlining each wear facet with a surface curve and then cutting it from the 3D tooth mesh (d). The area of the wear facet can then be calculated by the software

conducted in R statistical software (v.3.3.1). The potential for agreement between two methods will depend on the repeatability of each measurement (Bland & Altman, 1986). Consequently, dental wear facet identification and area measurements were performed 10 times on the SfM and SLS models of a single specimen. Each of these measurement sets was obtained on a different day. The absolute and relative technical error of measurement (TEM) were calculated for the repeated SfM and SLS facet area measurements using the method outlined by Langley et al. (2018).

3 | RESULTS

3.1 | Visual comparison

The surfaces of the SfM models were characterized by a high level of point redundancy and noise across the occlusal surface resulting in a 3D mesh in which the boundary of dental wear facets and other topographic features were poorly defined (Figure 4). The surface details on the 3D models generated using FS-SfM were characterized by high levels of surface noise and extremely high point densities. Despite this, the definition of surface features, particularly the boundaries of dental wear facets, were slightly enhanced on the FS-SfM models relative to those derived using conventional SfM (Figure 5).

3.2 | Comparison of overall dimensions

Photogrammetric model generation using the camera rig for image capture resulted in models of consistent and replicable quality. The mean difference between replicate photogrammetric models ranged from 59 to 90 μm (Figure 6). The deviation between matched SLS and SfM point clouds was relatively low with mean differences between aligned point clouds ranging from 57 to 159 μm (Figures 4 and 6). Focus stacking did not result in 3D models that more closely approximate the overall dimensions of the SLS reference models (Figure 6).

3.3 | Cross-sectional area and macrowear patterns

The mean difference between measurements of crown cross-section area between SfM and SLS models did not differ significantly (Table 3). Most values fell within the 95% limits of agreement (Figure 7). Crown cross-section area differed significantly between FS-SfM and the SLS reference models, however, the percentage error was similar for the FS-SfM models and SfM models (Figure 7). Wear facet area measurements were significantly larger in the SfM models than in the reference SLS models (Table 3). The percentage error was 101% (Figure 7). Wear facet area measurements also differed significantly between the FS-SfM and SLS models, however,
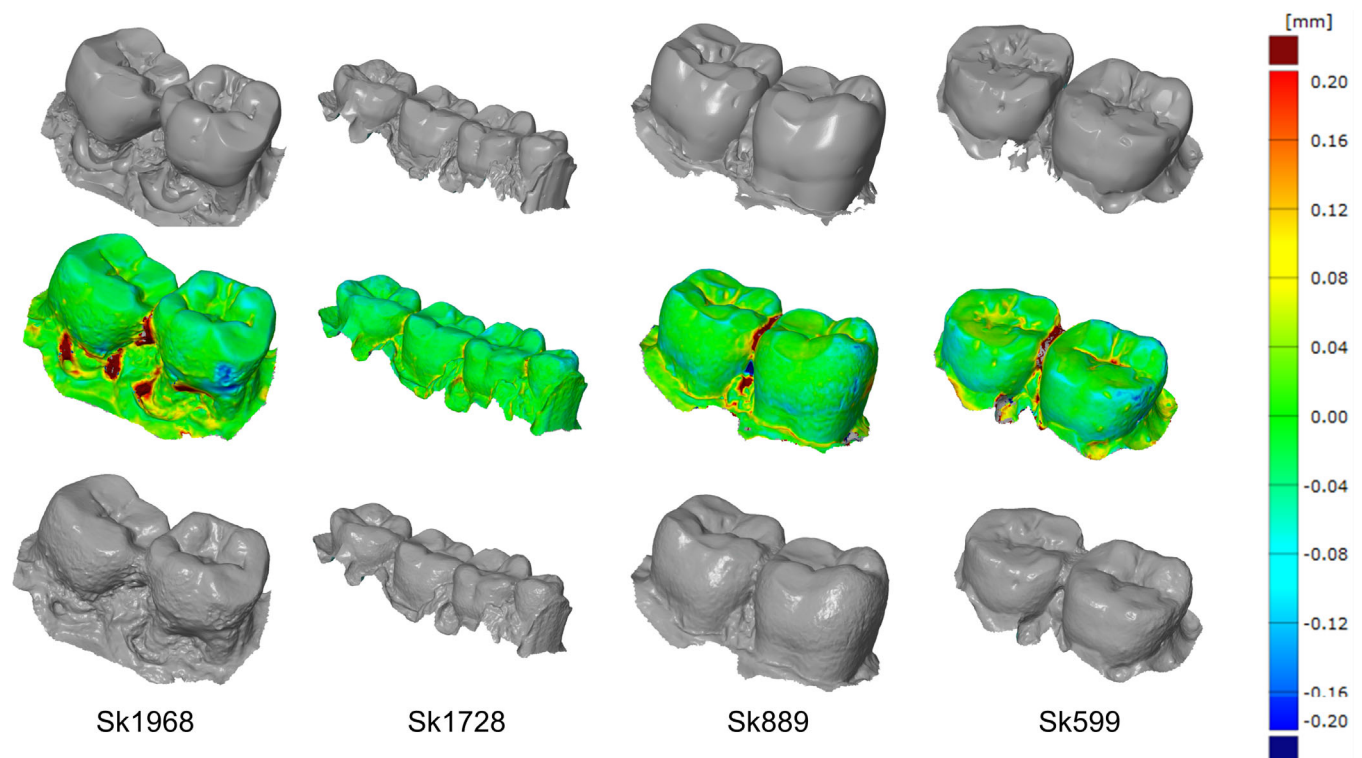

FIGURE 4 Examples of SfM (Lower row) and SLS versions (Upper row) of four 3D dental models. The central row presents visualizations of the distances between the aligned meshes expressed using the color scale on the right
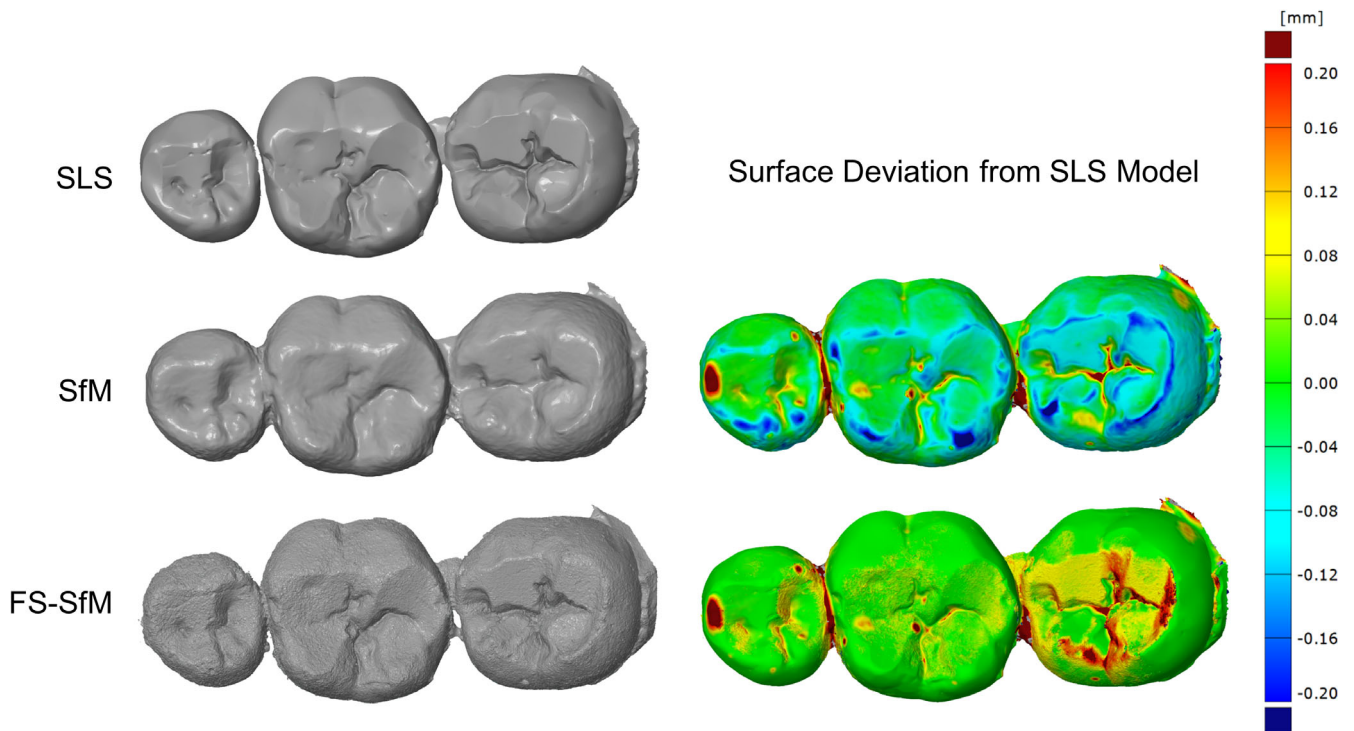
FIGURE 5 Occlusal view of 3D models of SK4293 generated using structured light scanning (SLS), structure-from-motion photogrammetry (SfM) and focus stacked structure-from-motion photogrammetry (FS-SfM). The surface deviation between the SfM and SLS model and the FS-SfM and SLS model is visualized in the images on the right using the color ramp
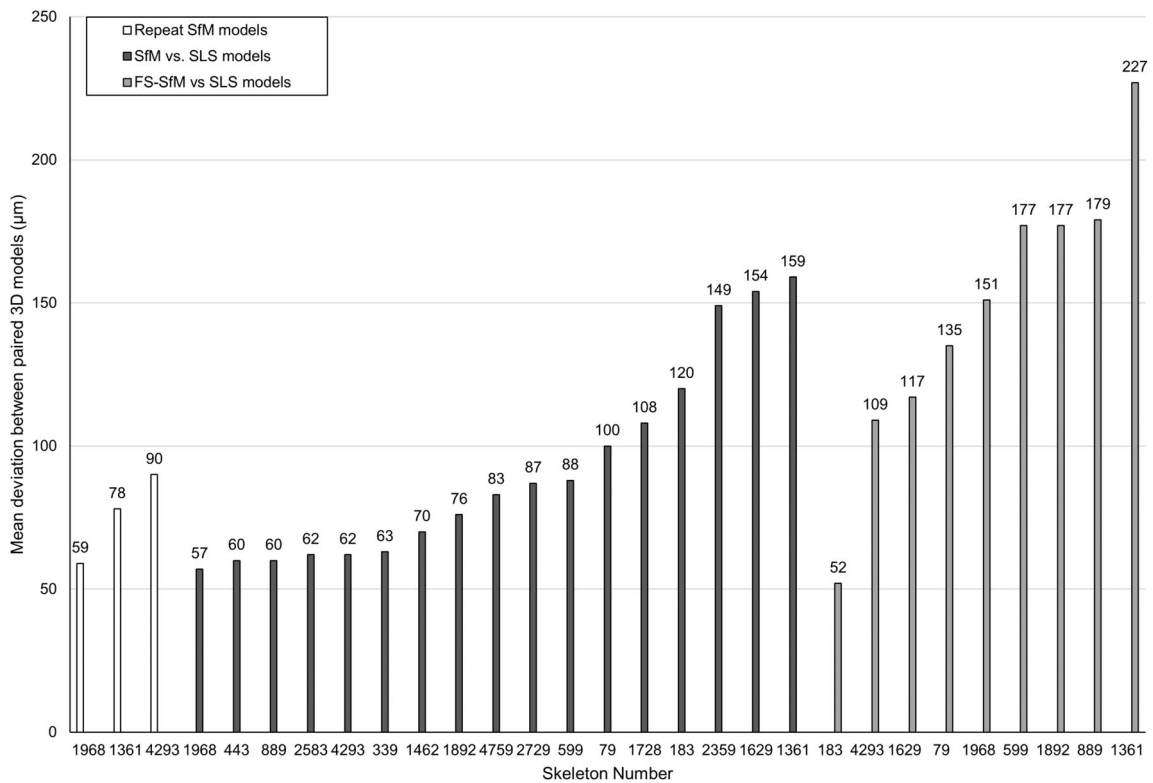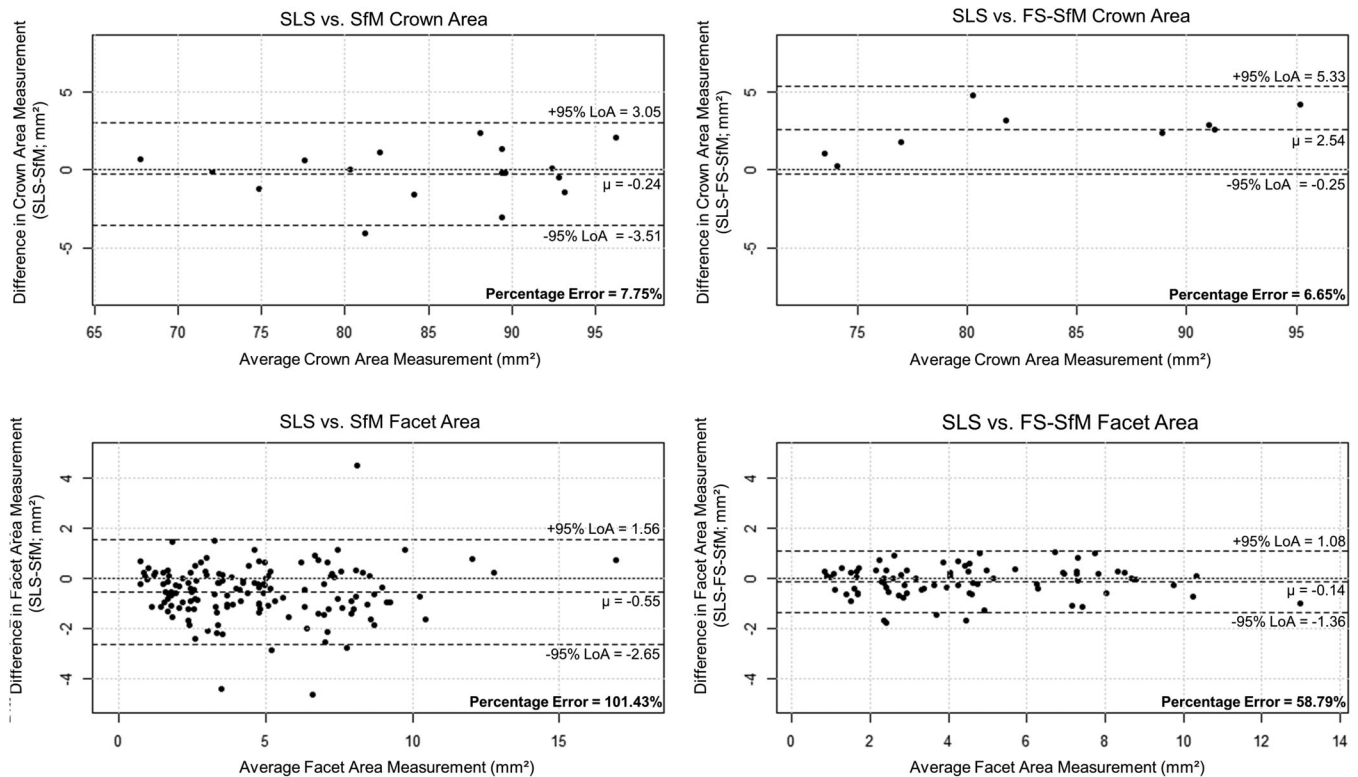

FIGURE 6 Bar chart showing the mean difference between aligned replicate Structure-from-motion (SfM) 3D models (white), the mean difference between 3D models generated using Structure-from-Motion and structured light scanning (SLS) (dark gray) and the mean difference between 3D models generated using Focus stacked Structure-from-Motion and structured light scanning (SLS) (light gray)

TABLE 3 Results of paired sample t-tests comparing crown areas and wear facet areas measurements derived using photogrammetric dental models and the SLS reference models

Comparison	t	Df	p-value	Mean difference	95% CI lower	95% CI upper
SfM vs SLS crown area	−0.59	16	.56	−0.24	−1.10	0.62
FS-SfM vs SLS crown area	5.15	8	<.001	2.54	1.75	4.57
SfM vs SLS facet area	−6.10	143	<.001	−0.55	−0.72	−0.37
FS-SfM vs SLS facet area	2.02	78	.05	0.14	0.002	0.28

FIGURE 7 Bland–Altman plots illustrating the distribution of differences between crown area measurements (mm²) of SLS and SfM models (upper left); crown area measurements (mm²) of SLS and FS-SfM models (upper right); wear facet area measurements (mm²) of SLS and SfM models (lower left); wear facet area measurements (mm²) of SLS and FS-SfM models (lower right). The upper and lower 95% limits of agreement (LoA) are given

the magnitude of this difference was smaller (Table 3; Figure 7). The percentage error figure was markedly less when comparing differences in cross-sectional crown area measurements relative to differences in wear facet area measurement. In addition, 10 of the wear facets evident in the gypsum model and the SLS model could not be identified in the SfM model due to the poor quality of the occlusal surface detail.

Relative TEM was markedly larger when measuring and identifying occlusal wear facets in the SfM models (8.21%) when compared to the SLS models (1.36%). The mean measurements for wear facet area were not significantly different between the 10 repeated sets of measurements for the photogrammetric models (Repeated measures ANOVA, F [df = 4.50] = 1.89, p = .11), however, the magnitude of difference between the means of repeated measurement sets was

smaller for the SLS models (Repeated measure ANOVA, F [df = 3.65] =0.57, p = .67).

4 | DISCUSSION

4.1 | Approximation of overall surface morphology

Overall tooth shape was captured effectively using SfM photogrammetry and supports previous studies that have found relatively low levels of deviation between point clouds of small objects derived from SfM and SLS systems (<100 μm) (Kontogianni, Chliverou, Georgopoulos, et al., 2017; Kontogianni, Chliverou, Koutsoudis, et al., 2017). The virtual 3D models generated using SfM were of

relatively consistent quality and could be readily replicated due to the production of a camera rig that ensured the sequence and distribution of image capture was highly repeatable. The close approximation of the overall size and shape of the SfM virtual models is close to the 0.1 mm accuracy that has been suggested as necessary for virtual models to have diagnostic value for clinical treatment (Fu et al., 2017; Taneva et al., 2015).

4.2 | The use of SfM models to derive metric data

Cross-sectional crown areas derived from the SfM models did not differ significantly from the measurements taken on the SLS reference models indicating that overall crown dimensions can be assessed using photogrammetric models. The significant difference between crown area measurements for the FS-SfM models and the SLS models indicates that the non-focus stacked method of SfM model generation used may more accurately reconstruct the overall geometry of the target teeth.

Previous studies have highlighted the potential for photogrammetry to closely preserve object geometry and yield measurements comparable to those derived from 3D models produced using high resolution scanning techniques (Fourie, Damstra, Gerrits, & Ren, 2011; Katz & Friess, 2014). Despite the high levels of repeatability and the capacity of SfM models to approximate closely the overall size and shape of teeth, the representation of small scale details of the occlusal topography and dental wear patterns was poor when compared to the 3D reference models. This is consistent with the study by Evin et al. (2016) which found that the tooth rows of wolf crania were captured in more detail using an SLS system rather than photogrammetry. There was a tendency to overestimate facet size where boundaries were difficult to define in the SfM models due to high levels of surface noise. This likely impacted the 3D dental wear facets area measurements. In addition, the identification of several facets, typically less than 1.5 mm^2 in area, was frequently not possible on the SfM models. The substantially lower levels of repeatability for SfM facet identification also will have contributed to the large percentage error figure obtained when conducting the Bland–Altman comparison.

The large relative TEM for wear facet area measurement in the SfM models was beyond the level of acceptability for repeated measures of metrics (>1.5%) (Langley et al., 2018). The deviation between wear facet area derived from the SfM and SLS models exceeded the magnitude of variation between individuals and assemblages examined in previous OFA studies (e.g., Fiorenza et al., 2011) suggesting that SfM, when conducted using the methods outlined in the current study, does not yield virtual models of adequate quality for the analysis of dental macrowear patterns. The 3D models generated using FS-SfM captured slightly higher levels of detail on the occlusal surface. This slightly improved the accuracy of wear facet identification and measurement, however, high levels of surface noise meant that the deviation of these measurements from those derived from the SLS reference models was

still beyond the limits of acceptability for the performance of OFA. Similarly, although studies of 3D topographic changes in the geosciences have reported the capacity of SfM approaches to detect changes in the profile of surfaces at a submillimetre level, the detection of scratches and features smaller than 0.3 mm was inconsistent and fell outside the limits of detection of the method used in a recent study (Cullen, Verma, & Bourke, 2018).

4.3 | Current limitations of SfM and future directions

As a passive technique of non-contact surface scanning, the resolution of 3D reconstructions that utilize photogrammetry are directly dependent upon the texture of the target object. In contrast, the deformation of the structured light pattern projected onto the object's surface by SLS systems enables the accurate estimation of 3D object geometry largely irrespective of limited variability in object texture (Errickson et al., 2017; Salvi et al., 2010). Although the use of dental gypsum overcomes issues associated with the reflective properties of dental enamel, the surface of gypsum exhibits a uniform color and texture. In addition, teeth are characterized by areas lacking textural variation alongside areas with textural variation occurring at a very small-scale, compounding this issue. This may limit the potential for passive non-contact imaging techniques to locate correspondences between images. Projecting a textured light pattern onto dental gypsum models whilst performing photogrammetry has been shown to result in more accurate 3D models that more closely approximate the output of an SLS system (Santoši et al., 2018).

Focus stacking was associated with a slight increase in the quality of the capture of surface details using the method employed in the current study when compared to conventional SfM. The boundaries of dental wear facets were more clearly defined, however, high levels of surface noise, associated with an extremely high point density, hindered the accurate quantification of the wear pattern. Extensive mesh decimation and smoothing would be required for use in Occlusal Fingerprint Analysis, which may have detrimental effects on topology and measurements (Veneziano, Landi, & Profico, 2018). High quality 3D models have been generated of extremely small insect specimens (1.5 mm body size) using focus stacked photogrammetry, however, these results were achieved using a complex workflow and largely automated systems (Nguyen, Lovell, Adcock, & La Salle, 2014; Ströbel, Schmelzle, Blüthgen, & Heethoff, 2018). The high input of time needed for capturing and processing the images required for focus stacking (Gallo et al., 2014) renders it impractical for the generation of large numbers of 3D dental models without access to a specially designed automated system. A structured light scanning system provides a more rapid and detailed surface acquisition method where available.

SfM provides a method for generating virtual dental models of consistent quality that closely approximate the size and shape of those derived from SLS systems. The limited deviation between the SfM and SLS point clouds supports the utility of SfM models in

making limited metric assessments of small topographically complex objects, such as deriving cross-sectional tooth crown areas. The very high quality of virtual models required to analyze small-scale details on the occlusal surface of teeth, however, cannot be satisfied by SfM in the forms presented in the current study as fine surface details (<100 μm) are not effectively visualized. Further innovation and methodological experimentation are required to determine whether photogrammetric model quality can be enhanced to produce high fidelity 3D models of small topographically complex objects that emulate the output of high resolution scanners.

CONFLICT OF INTEREST

No conflict of interest has been declared by the authors.

AUTHOR CONTRIBUTIONS

Christopher Silvester: Conceptualization; data curation; formal analysis; funding acquisition; investigation; methodology; resources; software; validation; visualization; writing-original draft; writing-review and editing. **Simon Hillson:** Conceptualization; formal analysis; funding acquisition; investigation; methodology; resources; software; supervision; writing-original draft; writing-review and editing.

DATA AVAILABILITY STATEMENT

The data that support the findings will be available in figshare following an embargo from the date of publication to allow for the completion of dissertation research. SfM photogrammetry: Photographs (DOI: 10.5522/04/9939473; DOI: 10.5522/04/9939419; DOI: 10.5522/04/9939344; DOI: 10.5522/04/9939290) and 3D models (DOI: 10.5522/04/9934346). Focus stacked SfM photogrammetry: Photographs (DOI:10.5522/04/9939611) and 3D models (DOI: 10.5522/04/9939533) SLS 3D models (DOI: 10.5522/04/9934442).

ORCID

Christopher Martin Silvester https://orcid.org/0000-0003-2843-1921

REFERENCES

Allen, K. L., Cooke, S. B., Gonzales, L. A., & Kay, R. F. (2015). Dietary inference from upper and lower molar morphology in Platyrrhine primates. *PLoS One*, *10*(3), e0118732. https://doi.org/10.1371/journal.pone.0118732

Bevan, A., Li, X., Martinón-Torres, M., Green, S., Xia, Y., Zhao, K., & Rehren, T. (2014). Computer vision, archaeological classification and China's terracotta warriors. *Journal of Archaeological Science*, *49*(1), 249–254. https://doi.org/10.1016/j.jas.2014.05.014

Bland, J. M., & Altman, D. (1986). Statistical methods for assessing agreement between two methods of clinical measurement. *The Lancet*, *327* (8476), 307–310. https://doi.org/10.1016/S0140-6736(86)90837-8

Bunn, J. M., & Ungar, P. S. (2009). Dental topography and diets of four old world monkey species. *American Journal of Primatology*, *71*(6), 466–477. https://doi.org/10.1002/ajp.20676

Clini, P., Nespeca, N., Ruggeri, M., Frapiccini, R., & Mengoni, L. (2016). SFM technique and focus stacking for digital documentation of archaeological artifacts. *International Archives of the Photogrammetry, Remote Sensing and Spatial Information Sciences*, *41*, 229–236. https://doi.org/10.5194/isprs-archives-XLI-B5-229-2016

Cullen, N. D., Verma, A. K., & Bourke, M. C. (2018). A comparison of structure from motion photogrammetry and the traversing micro-erosion meter for measuring erosion on shore platforms. *Earth Surface Dynamics*, *6*, 1023–1039. https://doi.org/10.5194/esurf-6-1023-2018

Delaunoy, A., Prados, E., Piracés, P.G.I., Pons, J.P., & Sturm, P. (2008). Minimizing the multi-view stereo reprojection error for triangular surface meshes. Paper presented at British machine vision conference, pp. 1–10.

Errickson, D., Grueso, I., Griffith, S. J., Setchell, J. M., Thompson, T. J. U., Thompson, C. E. L., & Gowland, R. L. (2017). Towards a best practice for the use of active non-contact surface scanning to record human skeletal remains from archaeological contexts. *International Journal of Osteoarchaeology*, *27*(4), 650–661. https://doi.org/10.1002/oa.2587

Evans, A. R., Wilson, G. P., Fortelius, M., & Jernvall, J. (2007). High-level similarity of dentitions in carnivorans and rodents. *Nature*, *445*(7123), 78–81. https://doi.org/10.1038/nature05433

Evin, A., Souter, T., Hulme-Beaman, A., Ameen, C., Allen, R., Viacava, P., ... Dobney, K. (2016). The use of close-range photogrammetry in zoo-archaeology: Creating accurate 3D models of wolf crania to study dog domestication. *Journal of Archaeological Science: Reports*, *9*, 87–93. https://doi.org/10.1016/j.jasrep.2016.06.028

Fiorenza, L., Benazzi, S., & Kullmer, O. (2009). Morphology, wear and 3D digital surface models: Materials and techniques to create high-resolution replicas of teeth. *Journal of Anthropological Sciences*, *87*, 211–218. http://www.isitaorg.com/jass/Contents/2009%20vol87/PDF/On-Line_bassa/JASs2009_09_Fiorenza.pdf

Fiorenza, L., Benazzi, S., Tausch, J., Kullmer, O., Bromage, T., Schrenk, F., & Rosenberg, K. (2011). Molar macrowear reveals Neanderthal eco-geographic dietary variation (Neanderthal tooth Wear). *PLoS One*, *6*(3), E14769. DOI: https://doi.org/10.1371/journal.pone.0014769, e14769.

Fiorenza, L., & Kullmer, O. (2013). Dental Wear and cultural behavior in middle Paleolithic humans from the near east. *American Journal of Physical Anthropology*, *152*(1), 107–117. https://doi.org/10.1002/ajpa.22335

Fiorenza, L., Benazzi, S., Oxilia, G., & Kullmer, O. (2018). Functional relationship between dental macrowear and diet in late Pleistocene and recent modern human populations. *International Journal of Osteoarchaeology*, *28*(2), 153–161. https://doi.org/10.1002/oa.2642

Fiorenza, L., Yong, R., Ranjitkar, S., Hughes, T., Quayle, M., McMenamin, P. G., ... Adams, J. W. (2018). Technical note: The use of 3D printing in dental anthropology collections. *American Journal of Physical Anthropology*, *167*(2), 400–406. https://doi.org/10.1002/ajpa.23640

Fourie, Z., Damstra, J., Gerrits, P. O., & Ren, Y. (2011). Evaluation of anthropometric accuracy and reliability using different three-dimensional scanning systems. *Forensic Science International*, *207*(1), 127–134. https://doi.org/10.1016/j.forsciint.2010.09.018

Fu, X., Peng, C., Li, Z., Liu, S., Tan, M., & Song, J. (2017). The application of multi-baseline digital close-range photogrammetry in three-dimensional imaging and measurement of dental casts. *PLoS One*, *12* (6), e0178858. https://doi.org/10.1371/journal.pone.0178858

Gallo, A., Muzzupappa, M., & Bruno, F. (2014). 3D reconstruction of small sized objects from a sequence of multi-focused images. *Journal of Cultural Heritage*, *15*(2), 173–182. https://doi.org/10.1016/j.culher.2013.04.009

Gargallo, P., Prados, E., & Sturm, P. (2007). Minimizing the reprojection error in surface reconstruction from images. Paper presented at IEEE 11th international conference on computer vision, pp. 1–8.

Geng, J. (2011). Structured-light 3D surface imaging: A tutorial. *Advances in Optics and Photonics*, *3*(2), 128–160. https://doi.org/10.1364/AOP.3.000128

Glowacka, H., Mcfarlin, S., Catlett, K., Mudakikwa, A., Bromage, T., Cranfield, M. R., ... Schwartz, G. (2016). Age-related changes in molar topography and shearing crest length in a wild population of mountain gorillas from volcanoes National Park, Rwanda. *American Journal of Physical Anthropology*, *160*(1), 3–15. https://doi.org/10.1002/ajpa.22943

Hassett, B., & Lewis-Bale, T. (2017). Comparison of 3D landmark and 3D dense cloud approaches to Hominin mandible Morphometrics using structure-from-motion. *Archaeometry*, *59*(1), 191–203. https://doi.org/10.1111/arcm.12229

HeliconSoft. (2019). Understanding the focus stacking parameters. Retrieved from https://www.heliconsoft.com/helicon-focus-main-parameters/

Hess, M., MacDonald, L., & Valach, W. (2018). Application of multi-modal 2D and 3D imaging and analytical techniques to document and examine coins on the example of two Roman silver denarii. *Heritage Science*, *6*(1), 1–22. https://doi.org/10.1186/s40494-018-0169-2

James, M., & Robson, S. (2012). Straightforward reconstruction of 3D surfaces and topography with a camera: Accuracy and geoscience application. *Journal of Geophysical Research*, *117*, F03017. https://doi.org/10.1029/2011JF002289

James, M., & Robson, S. (2014). Mitigating systematic error in topographic models derived from UAV and ground-based image networks. *Earth Surfaces Processes and Landforms*, *39*(10), 1413–1420. https://doi.org/10.1002/esp.3609

Kaidonis, J. (2008). Tooth wear: The view of the anthropologist. *Clinical Oral Investigations*, *12*(S1), 21–26. https://doi.org/10.1007/s00784-007-0154-8

Kaiser, T., Müller, D., Fortelius, M., Schulz, E., Codron, D., & Clauss, M. (2013). Hypsodonty and tooth facet development in relation to diet and habitat in herbivorous ungulates: Implications for understanding tooth wear. *Mammal Review*, *43*(1), 34–46. https://doi.org/10.1111/j.1365-2907.2011.00203.x

Katz, D., & Friess, M. (2014). 3D from standard digital photography of human crania-a preliminary assessment. *American Journal of Physical Anthropology*, *154*(1), 152–158. https://doi.org/10.1002/ajpa.22468

Klukkert, Z. S., Teaford, M. F., & Ungar, P. S. (2012). A dental topographic analysis of chimpanzees. *American Journal of Physical Anthropology*, *148*(2), 276–284. https://doi.org/10.1002/ajpa.21592

Koenigswald, W. (2018). Specialized wear facets and late ontogeny in mammalian dentitions. *Historical Biology*, *30*(1–2), 7–29. https://doi.org/10.1080/08912963.2016.1256399

Kontogianni, G., Chliverou, R., Koutsoudis, A., Pavlidis, G., & Georgopoulos, A. (2017). Enhancing close-up image based 3d digitisation with focus stacking. *The International Archives of the Photogrammetry, Remote Sensing and Spatial Information Sciences*, *42*(2), 421–425. https://doi.org/10.5194/isprs-archives-XLII-2-W5-421-2017

Kontogianni, G., Chliverou, R., Georgopoulos, A., Koutsoudis, A., & Pavlidis, G. (2017). Investigating the effect of focus stacking on sfm-mvs algorithms. *The International Archives of the Photogrammetry, Remote Sensing and Spatial Information Sciences*, *42*(2), 385–389. https://doi.org/10.5194/isprs-archives-XLII-2-W3-385-2017

Kullmer, O., Benazzi, S., Fiorenza, L., Schulz, D., Bacso, S., & Winzen, O. (2009). Technical note: Occlusal fingerprint analysis: Quantification of tooth wear pattern. *American Journal of Physical Anthropology*, *139*(4), 600–605. https://doi.org/10.1002/ajpa.21086

Kullmer, O., Benazzi, S., Schulz, D., Gunz, P., Kordos, L., & Begun, D. R. (2013). Dental arch restoration using tooth macrowear patterns with application to Rudapithecus hungaricus, from the late Miocene of Rudabánya, Hungary. *Journal of Human Evolution*, *64*(2), 151–160. https://doi.org/10.1016/j.jhevol.2012.10.009

Langley, N. R., Jantz, L. M., Mcnulty, S., Maijanen, H., Ousley, S. D., & Jantz, R. L. (2018). Data for validation of osteometric methods in forensic anthropology. *Data in Brief*, *19*, 21–28. https://doi.org/10.1016/j.dib.2018.04.148

Luhmann, T., Robson, S., Kyle, S., & Boehm, J. (2013). *Close-range photogrammetry and 3D imaging*. Berlin, Boston: De Gruyter.

M'Kirera, F., & Ungar, P. S. (2003). Occlusal relief changes with molar wear in *Pan troglodytes* troglodytes and *Gorilla gorilla* gorilla. *American Journal of Physical Anthropology*, *60*(2), 31–41. https://doi.org/10.1002/ajp.10077

Micheletti, N., Chandler, J. H., & Lane, S. N. (2015). Investigating the geomorphological potential of freely available and accessible structure-from-motion photogrammetry using a smartphone. *Earth Surface Processes and Landforms*, *40*(4), 473–486. https://doi.org/10.1002/esp.3648

Morgan, J. A., Brogan, D. J., & Nelson, P. A. (2017). Application of structure-from-motion photogrammetry in laboratory flumes. *Geomorphology*, *276*, 125–143. https://doi.org/10.1016/j.geomorph.2016.10.021

Morgan, B., Ford, A., & Smith, M. (2019). Standard methods for creating digital skeletal models using structure-from-motion photogrammetry. *American Journal of Physical Anthropology*, *169*(1), 152–160. https://doi.org/10.1002/ajpa.23803

Mosbrucker, A., Major, J., Spicer, K., & Pitlick, J. (2017). Camera system considerations for geomorphic applications of SfM photogrammetry. *Earth Surface Processes and Landforms*, *42*(6), 969–986. https://doi.org/10.1002/esp.4066

Napolitano, R. K., & Glisic, B. (2018). Minimizing the adverse effects of bias and low repeatability precision in photogrammetry software through statistical analysis. *Journal of Cultural Heritage*, *31*, 46–52. https://doi.org/10.1016/j.culher.2017.11.005

Nguyen, C. V., Lovell, D. R., Adcock, M., & La Salle, J. (2014). Capturing natural-colour 3D models of insects for species discovery and diagnostics. *PLoS One*, *9*(4), E94346. https://doi.org/10.1371/journal.pone.0094346

Salvi, J., Fernandez, S., Pribanic, T., & Llado, X. (2010). A state of the art in structured light patterns for surface profilometry. *Pattern Recognition*, *43*(8), 2666–2680. https://doi.org/10.1016/j.patcog.2010.03.004

Santoši, Ţ., Budak, I., Šokac, M., Puškar, T., Vukelić, Đ., & Trifković, B. (2018). 3D digitization of featureless dental models using close range photogrammetry aided by noise based patterns. *Facta Universitatis Series: Mechanical Engineering*, *16*(3), 297–305. https://doi.org/10.22190/FUME170620029S

Ströbel, B., Schmelzle, S., Blüthgen, N., & Heethoff, M. (2018). An automated device for the digitization and 3D modelling of insects, combining extended-depth-of-field and all-side multi-view imaging. *ZooKeys*, *759*(759), 1–27. https://doi.org/10.3897/zookeys.759.24584

Szeliski, R. (2011). *Computer vision. Algorithms and applications*. New York: Springer. https://doi.org/10.1007/978-1-84882-935-0

Taneva, E., Kusnoto, B., & Evans, C. (2015). Chapter 9: 3D scanning, imaging, and printing in orthodontics. In F. Bourzgui (Ed.), *Issues in contemporary orthodontics* (pp. 147–188). London, UK: IntechOpen. https://doi.org/10.5772/60010

Ulhaas, L., Kullmer, O., Schrenk, F., & Henke, W. (2004). A new 3-d approach to determine functional morphology of cercopithecoid molars. *Annals of Anatomy*, *186*(5), 487–493. https://doi.org/10.1016/S0940-9602(04)80090-6

Ungar, P. S., Healy, C., Karme, A., Teaford, M. F., & Fortelius, M. (2018). Dental topography and diets of platyrrhine primates. *Historical Biology*, *30*(1–2), 64–75. https://doi.org/10.1080/08912963.2016.1255737

Veneziano, A., Landi, F., & Profico, A. (2018). Surface smoothing, decimation, and their effects on 3D biological specimens. *American Journal of Physical Anthropology*, *166*(2), 473–480. https://doi.org/10.1002/ajpa.23431

Westoby, M. J., Brasington, J., Glasser, N. F., Hambrey, M. J., & Reynolds, J. M. (2012). Structure-from-motion' photogrammetry: A low-cost, effective tool for geoscience applications. *Geomorphology*, *179*, 300–314. https://doi.org/10.1016/j.geomorph.2012.08.021